Ye Li, Wei Cao, Lunlun Gong, Ruifang Zhang and Xudong Cheng*

Effect of Starch on Sintering Behavior for Fabricating Porous Cordierite Ceramic

DOI 10.1515/htmp-2015-0074
Received March 25, 2015; accepted October 16, 2015

Abstract: Porous cordierite ceramics were prepared with starch as pore-forming agent by solid-state method. The green bodies were sintered at 1,100–1,400 °C for 2 h. The characterization was focused on thermal analysis, phase evolution, sintering behavior, porosity and micro-structural changes. The results show that cordierite becomes the main crystallization phase at 1,200 °C. The shrinkage behavior shows the most obvious dependence on the sintering temperature and starch content, and it can be divided into three stages. Moreover, the open porosity increases with the increase of starch content, but the pore-forming effectivity decreases. Nevertheless, compared with the open porosity curves, the bulk density curves are more in line with the linear rule. The microphotographs show the densification process with the sintering temperature and the variation of pore connectivity with the starch content.

Keywords: cordierite, porous ceramic, starch, sintering behavior, microstructure

Introduction

Cordierite ($2MgO{\cdot}2Al_2O_3{\cdot}5SiO_2$) is one of the most common industrial ceramics in many industrial applications. Cordierite ceramics have a lot of outstanding properties, such as excellent thermal shock resistance, high refractoriness, high mechanical strength, good chemical durability and low dielectric constant. So they are used as catalysts, microelectronics, refractory products, integrated circuit boards, heat exchanger for gas turbines, membranes, thermal shock-resistance tableware and porous ceramics [1, 2]. In recent years, porous ceramic has been widely concerned by researchers [3–6] and many preparation methods have been invented to improve the porosity of the ceramics. For example, the ceramics with more than 90 % porosity have been fabricated by sacrificial template [7] and direct foaming method [6, 8]. Ultrahigh porosity materials and their application are becoming a hot spot of research. However, the ceramic products with relatively moderate porosity (40–70 %) are still widely used and worthy to study. In our previous work, we have fabricated cordierite ceramic by solid-state method using kaolin, attapulgite and basic magnesium carbonate as the raw materials [9, 10]. Now starch was added as the pore-forming agent to further increase the porosity.

Ten years ago, starch had been used as a pore-forming agent in ceramic technology [11–14]. Moreover, starch can also serve as a body-forming agent called starch consolidation casting (SCC), due to its ability to swell in water at elevated temperatures, thus enabling ceramic green bodies to be fabricated by casting of suspensions with starch into non-porous molds (e. g. metal molds) [15–19]. However, most of researchers focused far more on the thermal, mechanical and electrical properties affected by the high porosity for the samples produced by added starch. Therefore, they usually sintered the green bodies with different starch contents at a constant temperature, which was the most favorable for the final properties. In this paper, we discussed the effect of the sintering temperature and starch content on the shrinkage, porosity, bulk density and microstructure, simultaneously. The shrinkage behavior shows the most obvious dependence on the sintering temperature and starch content, and it can be divided into three stages. The microstructure of the sintered samples also presents different forms based on the temperature and starch content.

Experimental

Materials and specimen preparation

Kaolin (chemically pure, Shanghai, China), attapulgite (Hebei, China) and basic magnesium carbonate (AR, Shanghai, China) were used as raw materials to

*Corresponding author: Xudong Cheng, State Key Laboratory of Fire Science, University of Science and Technology of China, Hefei, Anhui 230027, PR China, E-mail: chengxd@ustc.edu.cn
Ye Li, Wei Cao, Lunlun Gong, Ruifang Zhang, State Key Laboratory of Fire Science, University of Science and Technology of China, Hefei, Anhui 230027, PR China

Table 1: Elemental analysis of minerals using the X-ray fluorescence technique.

Attapulgite	MgO	Al_2O_3	SiO_2	Fe_2O_3	CaO	K_2O	TiO_2	MnO	P_2O_5	Others
wt %	7.1	10.7	69.3	7.5	2.1	1.3	1.2	0.16	0.31	0.33

synthesize cordierite. The chemical compositions of the raw materials were determined by X-ray fluorescence spectroscopy (XRF-1800, SHIMADZU, Japan) as shown in Table 1. Meanwhile, 5–30 wt.% of starch was employed as pore-forming agent. The above starting materials were mixed according to the chemical composition of cordierite with different contents of starch for 24 h in a high-energy planetary ball mill using alumina balls as media at a rotation speed of 180 rpm. After being dried at 105 °C in an oven and sieved through a 48-mesh screen, the powders for all the samples were mixed with 5 wt.% of polyvinyl alcohol (PVA) solution (AR, Shanghai, China), which was used as binder. In the above process, 4 ml of PVA solution was added into 30 g of the mixed powders and stirred evenly by glass rod in the beaker. Then, the mixture was pressed into cylindrical specimens with Φ25.5 mm × 5 mm under the pressure of 160 MPa using a steel die. The specimens were dried at 70 °C for 24 h and then sintered at 1,100–1,400 °C in air with a step of 50 °C. The dwell time at peak temperature was 2 h. The sintering schedule was defined by the added pore-forming agent.

Characterization techniques

The thermal behavior of the samples was studied by means of thermogravimetry (TG) and differential scanning calorimetry (DSC) methods using Netzsch STA 449CTG-DSC Jupiter Aeolos coupled to mass spectrometer from room temperature to 1,400 °C with a heating rate of 10 °C/min in air. The type of crystalline phases of the heat-treated samples were identified from X-ray diffraction (XRD) patterns, obtained using an X-ray diffractometer (X'Pert PRO, PHILIPS, 60 kV and 55 mA, α-monochromatic Cu-Kα radiation), in the $10° \le 2\theta \le 70°$. Linear firing shrinkage was simply calculated by measuring the diameter of the specimens before and after sintering. Bulk density and open porosity were determined by the Archimedes method using distilled water as liquid media. The microstructure of the thermally treated samples was observed on fracture surfaces by scanning electron microscopy (SEM) (JSM-6490LV, Japan).

Results and discussion

TG/DSC analysis

Figure 1 shows the TG–DSC curves of the green compacts of mixture without starch. At low temperature below 120 °C, there is an endothermic DSC peak at 47 °C with about 1.6 % mass loss, which is caused by the removal of physically adsorbed water. About 3.6 % mass loss of the mixture between 108 °C and 278 °C, accompanied with an endothermic DSC peak at 221.6 °C, can be ascribed to the dehydration of the crystal water. Due to the decomposition of basic magnesium carbonate, the third-stage mass loss starts at 278 °C and finishes at 499 °C with an endothermic DSC peak at 434 °C. There is a small mass loss about 0.65 % from 499 °C to 676 °C, which is caused by the transformation from kaolin to metakaolin [20, 21]:

$$Al_2O_3 \cdot 2SiO_2 \cdot 2H_2O \rightarrow Al_2O_3 \cdot 2SiO_2 + 2H_2O \uparrow$$

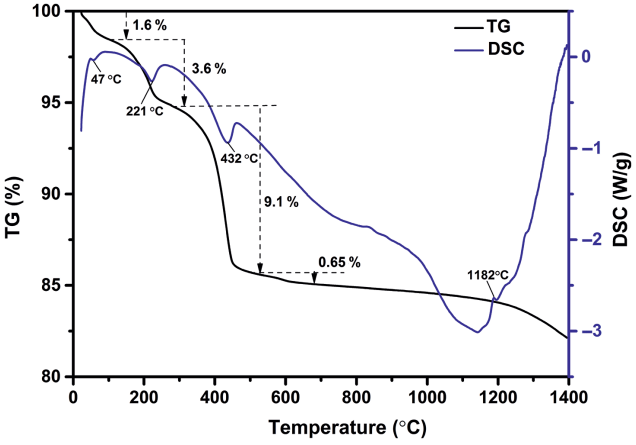

Figure 1: TG/DSC diagrams of the mixture without starch.

A small exothermic peak is observed at 1,182 °C, indicating phase transitions, which may be due to the production of cordierite based on the XRD results shown in Figure 3. The TG–DSC curves of starch are depicted in Figure 2 as well. There is also an endothermic DSC peak at 60 °C with about 11.5 % mass loss, resulting from the removal of physically adsorbed water. About 72.5 % mass

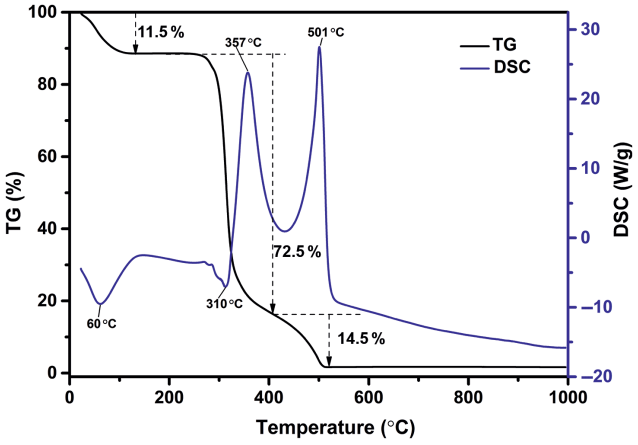

Figure 2: TG/DSC diagrams of starch.

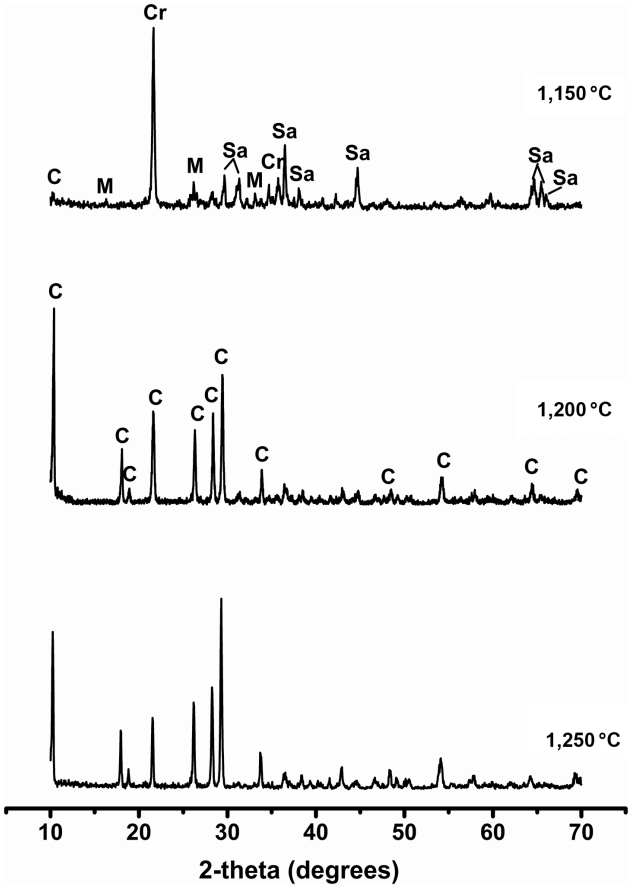

Figure 3: XRD patterns of the green compacts after sintering between 1,150 °C and 1,250 °C for 2 h.

loss of the starch from 188 °C to 411 °C, accompanied with an exothermic peak at 357 °C, can be ascribed to the heat degradation of starch. Whereafter the residue of the pyrolytic starch starts to burn, which is called glowing combustion, and finishes at 529 °C with an exothermic peak at 501 °C. Therefore, the green compacts were heated to 500 °C and held for 60 min to remove water and the organic additives. The heating rate was as slow as 2 °C/min to protect the samples from cracking. Then the samples were heated to the final temperatures by 5 °C/min of heating rate.

Phase transitions

Figure 3 shows the XRD patterns of the cordierite-based ceramics sintered at 1,150–1,250 °C for 2 h. There are four phases, including cristobalite, sapphirine, mullite and a small quantity of cordierite, at 1,150 °C. The crystalline phases of cristobalite and mullite can be ascribed to the reaction of kaolin to metakaolin by loss of crystallization of water and further decomposition into mullite and quartz, as shown in the following equation [22]:

$$3(Al_2O_3 \cdot 2SiO_2) \rightarrow 3Al_2O_3 \cdot 2SiO_2 + 4SiO_2$$

And the sapphirine phase may be a substituted cordierite with a composition shifted toward its primary field [23]. Moreover, as the sintering temperature increases to 1,200 °C, cordierite becomes the main phase, and the peak intensities of cristobalite, sapphirine and mullite phases decrease and almost approach to zero. This indicates that all the above phases react with each other to produce cordierite phase. Therefore, there is the small exothermic peak at 1,182 °C in the above DSC/TG curves (Section 3.1). The formation temperature of cordierite is slightly higher than that, which is 1,178 °C, for the mixture of the waste fly ash and $(MgCO_3)_4 \cdot Mg(OH)_2 \cdot 5H_2O$ based on the composition of cordierite by Dong [24]. Certainly, the formation temperature can be lower when other raw materials are used such as sepiolite/alumina [25] and kaolin/$Mg(OH)_2$ [26]. However, for the above three kinds of raw materials, cordierite does not appear abundantly until the temperature exceeds 1,300 °C. After 1,200 °C, there is little change for the crystalline phase except for the peak intensity.

Shrinkage

Figure 4 presents the diameter shrinkage percent of the cordierite compacts with different starch contents sintered at 1,150–1,400 °C for 2 h. For all the samples, the shrinkage percent increases with the increasing temperature. In general, the sintered shrinkage behavior of the samples results from the dehydration and decomposition of the organic additives before 1,000 °C [25], and then the particles of the raw materials connect to each other due

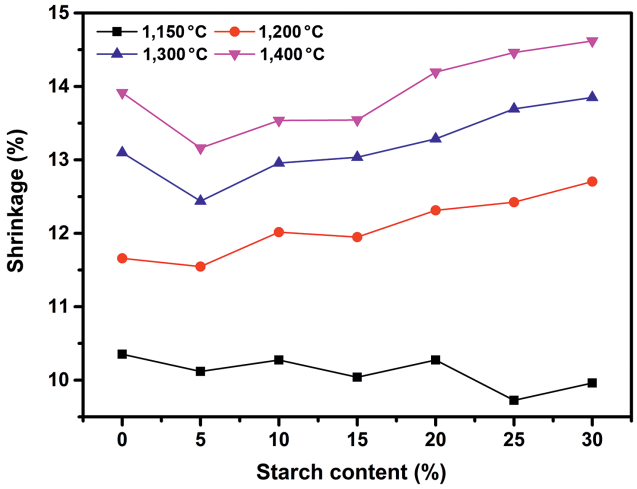

Figure 4: Comparison between shrinkage plots of samples with different starch contents.

to the formation of liquid glassy phase, resulting in a further shrinkage at high temperatures [27]. As shown in Figure 4, it is obvious that the shrinkage process can be divided into three stages based on the temperature. At 1,150 °C, the shrinkage percent of the sintered samples remains unchanged before 20 wt. % starch content and then slightly decreases. This may be the primary stage of the shrinkage process and the shrinkage mainly comes from the dehydration and decomposition of the organic additives. The pore-forming agent content has little effect on the diameter shrinkage percent and even when the content of pore-forming agent exceeds 25 wt. %, the pores left by the pore-forming agent prevent the shrinkage behavior of the samples. However, for the samples sintering at 1,200 °C, the shrinkage percent continues to increase with the starch content. This is the second stage, in which the particles connect to each other, forming the pieces of dense areas and pores (as shown in Figure 7). Meanwhile, parts of the small pores disappear due to the large amount of liquid glassy phase and the other pores merge with each other to produce the larger pores. The above processes result in a larger shrinkage [28], and the shrinkage effectiveness is affected by the content of starch with a positive correlation. When the samples are sintered at 1,300 °C and 1,400 °C, the shrinkage percent still increases when the starch content increases from 5 wt. % to 30 wt. %. But the shrinkage percent for the samples with 5–15 wt. % starch contents is lower than that for the samples without starch. In this stage, the effect of temperature on the shrinkage behavior gradually strengthens, and a denser ceramic substrate appears with larger pores. For the samples sintered at the same temperature, the percent of the large pores can impede the shrinkage process [29], resulting in the lower shrinkage percent of the samples with 5–15 wt. % starch contents. However, after the starch content increases up to 20 wt. %, the inhibition of the large pores to the shrinkage behavior loses efficacy relative to the acceleration effect of the starch content. Thus, the shrinkage percent starts to exceed that of the samples without starch.

Porosity and bulk density

Figure 5 shows the variation of open porosity in relation to the content of starch at different sintering temperatures (1,150–1,400 °C). For all the samples, the open porosity decreases with the temperature increasing from 1,150 °C to 1,400 °C. Moreover, as the starch content increases, the open porosity also increases. Based on the slopes of the curves, it can be observed that the increasing trend of the open porosity reduces especially after 15 wt. % starch content, indicating that the pore-forming effectivity decreases with the increase of starch content. Moreover, for the samples with the same starch content sintered between 1,150 °C and 1,400 °C, the different values of the open porosities decrease with the increasing starch content. As the samples are sintered from 1,150 °C to 1,400 °C, the densification process was enhanced, resulting in a significant reduction of the open porosity for all the starch contents. However, there is a smaller effect of the temperature on the open porosity for the samples with high open porosity.

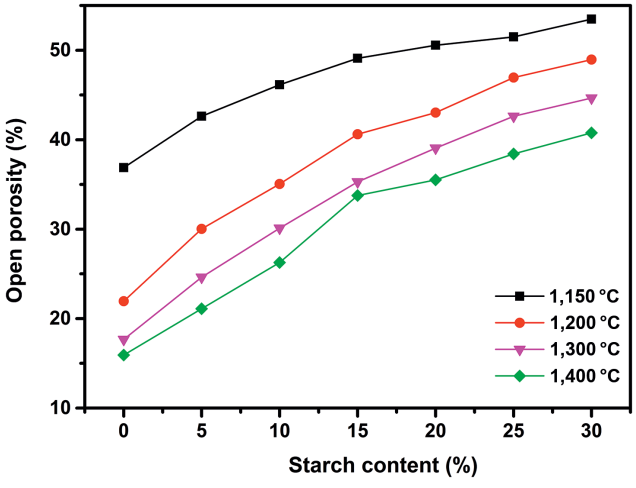

Figure 5: Comparison between porosity plots of samples with different starch contents.

Figure 6 shows the variation of bulk density in relation to the content of starch at different sintering temperatures

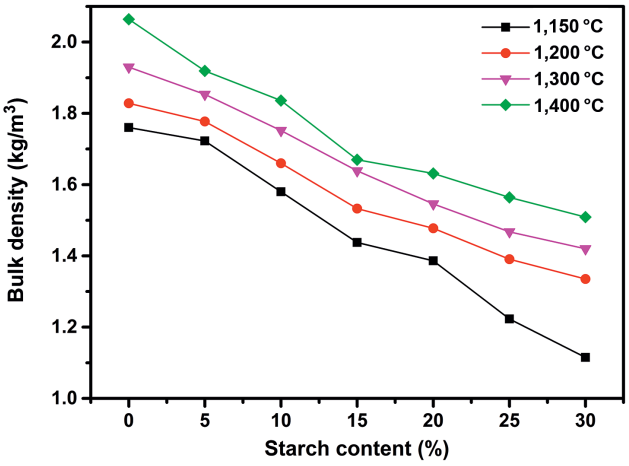

Figure 6: Comparison between bulk density plots of samples with different starch contents.

(1,150–1,400 °C). The bulk density decreases with the sintering temperature and starch content, respectively, which is in good agreement with open porosity. However, compared with the open porosity curves, the bulk density curves are more in line with the linear rule. This may be because that the density of the ceramic substrate can also affect the final bulk density except for the open porosity.

SEM microstructures

Figure 7 displays the SEM microphotographs of the porous cordierite samples without starch at 1,150 °C, 1,200 °C and 1,400 °C. It is found that the microstructures are extremely related to sintering temperature. With increasing sintering temperature, a gradual densification takes place because of the generation of more liquid glassy phase. As sintered at 1,150 °C, the neighboring particles connect with each other and form continuous small blocky areas, surrounded by small pores. When the temperature increases to 1,200 °C, it can be seen that the continuous small blocky areas are replaced by vast stretches of dense areas, and the small pores merge with each other to form large irregular holes. Whereafter, as the sintering temperature increases again, the dense areas further expands, accompanied by the disappearance of the small pores and the further growth of the large ones.

Figure 8 shows the SEM microphotographs of the porous cordierite samples with 5 wt.% and 20 wt.% starch contents at 1,200 °C and 1,400 °C. Comparing Figure 8(a) and (b), it can be found that with increasing

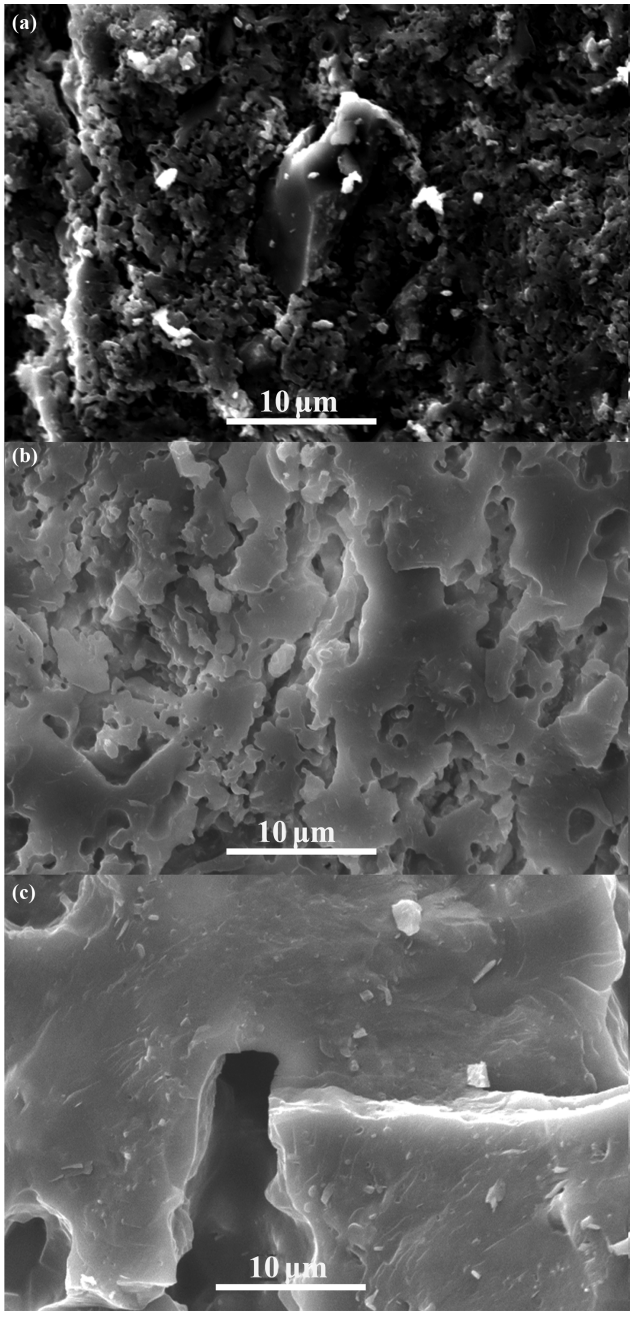

Figure 7: SEM microphotographs of the cordierite-based samples after sintering at 1,150 °C (a), 1,200 °C (b) and 1,400 °C (c) for 2 h without starch.

the starch content, the number of small blocky areas decreases obviously and large and spherical pores form. As the temperature increases to 1,400 °C, the shape of the pores for the samples with 5 wt.% starch content is spherical or ellipsoidal and part of the pores connected to each other. However, for the samples added 20 wt.% starch, the connectivity of the pores increases and the connecting pores similar to the river channels distribute

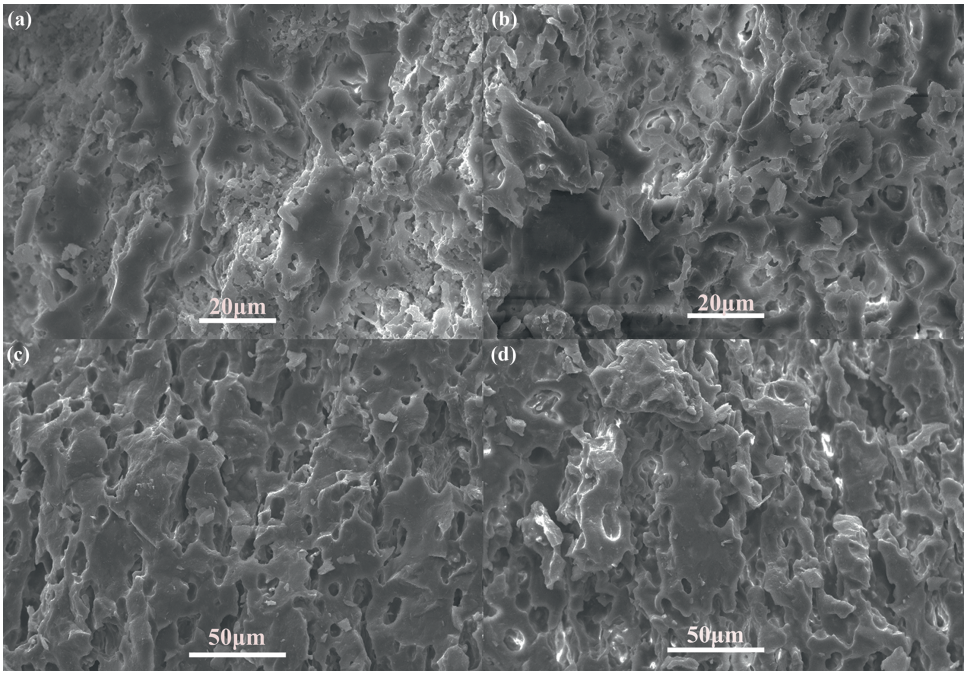

Figure 8: SEM microphotographs of the cordierite-based samples after sintering at 1,200 °C ((a)–(b)) and 1,400 °C ((c)–(d)) for 2 h with different starch contents: (a) and (c) 5 wt. %; (b) and (d) 20 wt. %.

in the ceramic substrate, which is divided into a number of islands.

Conclusions

Porous cordierite ceramics were prepared with starch as pore-forming agent by solid-state method. Cordierite becomes the main crystallization phase at 1,200 °C. The shrinkage behavior shows the most obvious dependence on the sintering temperature and starch content, and it can be divided into three stages. Moreover, for all the sintering temperatures, the open porosity of all increases with the increase in starch content and the variation of bulk density is also consistent with the porosity result. But the pore-forming effectivity decreases. From the SEM microphotographs, an obvious densification process of the ceramic substrate with sintering temperature and pore structure variation with starch content can be observed.

Funding: This work was supported by the National Basic Research Program of China (973 Program) (2012CB719701) and National Key Technology R&D Program of China (2013BAJ01B05).

References

[1] A. Chowdhury, S. Maitra, H.S. Das, A. Sen, G.K. Samanta and P. Datta, Int. Ceram. Rev., 56 (2007) 18–22.
[2] A.Chowdhury, S. Maitra, H.S. Das, A. Sen, G.K. Samanta and P. Datta, Int. Ceram. Rev., 56 (2007) 98–102.
[3] L.Dean-Mo, Ceram. Int., 24 (1998) 441–446.
[4] D.A. Hirschfeld, T.K. Li and D.M. Liu, Key Eng. Mater., 115 (1996) 65–80.
[5] H. Wang, X. Li, L.-Y. Hong and D.-P. Kim, J. Porous Mater., 13 (2006) 115–121.
[6] Y. Li, X. Cheng, L. Gong, J. Feng, W. Cao, R. Zhang and H. Zhang, J. Eur. Ceram. Soc., 35 (2015) 267–275.
[7] L. Andersson and L. Bergström, J. Eur. Ceram. Soc., 28 (2008) 2815–2821.
[8] Y. Han, C. Li, C. Bian, S. Li and C.-A. Wang, J. Eur. Ceram. Soc., 33 (2013) 2573–2578.
[9] Y. Li, X. Cheng, R. Zhang, Y. Wang and H. Zhang, Int. J. Appl. Ceram. Technol., 12 (2015) 443–450.
[10] Y. Li, H. Qian, X. Cheng, R. Zhang and H. Zhang, Mater. Lett., 116 (2014) 262–264.
[11] S.F. Corbin and P.S. Apte, J. Am. Ceram. Soc., 82 (1999) 1693–1701.
[12] A. Kristoffersson, J.B. Davis, E. Carlstrom, W.J. Clegg, J. Am. Ceram. Soc., 83 (2000) 2369–2374.
[13] J.-G. Kim, J.-H. Sim and W.-S. Cho, J. Phys. Chem. Solids, 63 (2002) 2079–2084.
[14] R. Barea, M.I. Osendi, J.M.F. Ferreira and P. Miranzo, Acta Mater., 53 (2005) 3313–3318.

[15] H.M. Alves, G. Tarì, A.T. Fonseca and J.M.F. Ferreira, Mater. Res. Bull., 33 (1998) 1439–1448.
[16] O. Lyckfeldt and J.M.F. Ferreira, J. Eur. Ceram. Soc., 18 (1998) 131–140.
[17] A.F. Lemos and J.M.F. Ferreira, Mater. Sci. Eng. C, 11 (2000) 35–40.
[18] E. Gregorová, Z. Živcová and W. Pabst, J. Mater. Sci., 41 (2006) 6119–6122.
[19] L. Gong, Y. Wang, X. Cheng, R. Zhang and H. Zhang, J. Porous Mater., 21 (2013) 15–21.
[20] Y.-F. Chen, M.-C. Wang and M.-H. Hon, J. Mater. Res., 18 (2003) 1355–1362.
[21] Y.-F. Chen, Y.-H. Chang, M.-C. Wangand M.-H. Hon, Mater. Sci. Eng. A, 373 (2004) 221–228.
[22] J. Banjuraizah, H. Mohamad and Z.A. Ahmad, Int. J. Appl. Ceram. Technol., 8 (2011) 637–645.
[23] M. Genevrier and A.Mocellin., J. Am. Ceram. Soc., 79 (1996) 2098–2104.
[24] Y. Dong, X. Liu, Q. Ma and G. Meng, J. Membr. Sci., 285 (2006) 173–181.
[25] J. Zhou, Y. Dong, S. Hampshire and G. Meng, Appl. Clay Sci., 52 (2011) 328–332.
[26] Y. Kobayashi, K. Sumi and E. Kato, Ceram. Int., 26 (2000) 739–743.
[27] Y. Dong, S. Hampshire, J.E. Zhou, B. Lin, Z. Ji, X. Zhang and G. Meng, J. Hazard Mater., 180 (2010) 173–180.
[28] S. Li, C.-A. Wang and J. Zhou, Ceram. Int., 39 (2013) 8833–8839.
[29] E. Gregorová and W. Pabst, J. Eur. Ceram. Soc., 31 (2011) 2073–2081.